E-21-6TH

"Novel High Efficiency Photovoltaic Devices Based on the III-N Material System"

January 28, 2005

Introduction

The theoretical efficiency limits of solar energy conversion are strongly dependant on the range and number of different band gaps or effective band gaps that can be incorporated into a solar cell. For tandem devices, the range of band gaps available as well as the ability to achieve junctions with specific band gaps and device structures is critical in achieving high efficiency. For alternate approaches, in which one or more of the band gaps are "effective band gaps" due to physical mechanisms such as an intermediate band, higher order excited states, or energy levels or bands introduced by quantum well or quantum dots, the need for specific band gaps is relaxed. However, in both approaches, both the low and the high band gaps are still controlled by the materials system. Consequently, the recent re-measurement of the band gap of InN as on the order of 0.7 eV makes the InGaN alloy system a potential solar cell material.

While band gaps figure prominently in determining efficiency limits, the ability to implement a practical, high efficiency device depends on many other parameters, including absorption, diffusion length, effect of surfaces, lattice constant, and doping. This report examines the ability to use InGaN for photovoltaic devices with the goal of determining if the InGaN material system can be used to make ultra-high efficiency (>50% efficiency) solar cells. The advantages of the III-nitride material system are a wide range in band gap, high absorption coefficient, a low effective mass (high mobility), and strong piezoelectric and polarization effects. However, in addition to these advantages, the material system also has significant challenges, some of which are related to the newness of the material, including material quality, defect density, doping, substrates and growth issues.

Growth and Characterization of In-rich InGaN

A paper entitled "Growth of InN on Ge Substrate by Molecular Beam Epitaxy" was submitted to the Journal of Crystal. It is currently under review. The paper described results from the first demonstration of growing InN on Ge substrate. InN was epitaxially grown on a (111) oriented, Ga-doped germanium substrate using molecular beam epitaxy. X-ray diffraction and transmission electron microscopy investigations showed that the InN epitaxial layer consists of a wurtzite structure, which has the epitaxial relationship of $(0002)_{InN}||(111)_{Ge}$.

X-ray diffraction of the InN (0002) found a FWHM ~360 arcsec for a 0.4μm thick film as shown in figure 1. This is equivalent to other research group results for 5-8 μm thick films. Transmission electron microscopy found an intermediate layer at the interface between the InN/Ge substrate. Consistent with recent reports implying a narrow bandgap of InN, a strong photoluminescence with peak energy of 0.69 eV at 15 K was observed for this InN epilayer, in contrast to the peak energy of 0.71 eV for Ga-doped Ge

under the same measurement conditions. We were able to demonstrate InN on Ge with a reasonably good quality.

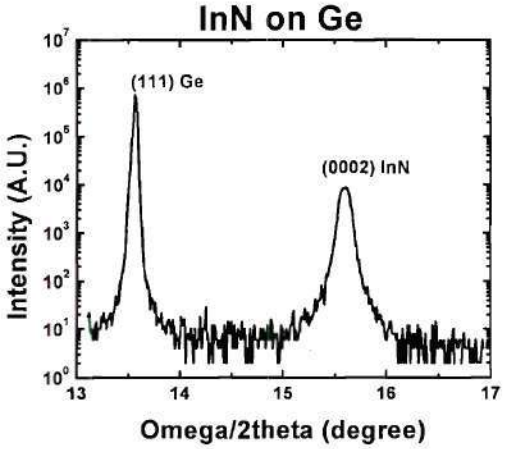

Fig. 1: X-Ray Diffraction of (0002) InN on (111) Ge

The current/voltage curves of InN/Ge showed an ohmic relationship as seen in figure 2. This may prove useful for creating tandem solar cells.

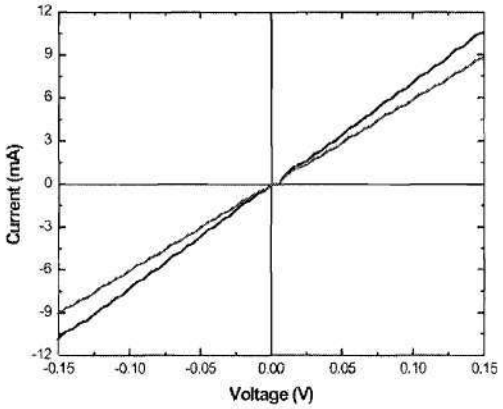

Fig. 2: I-V Characteristic of InN/Ge

Above is the IV curve for n-InN/p-Ge for 1x2mm (red) and 2x2mm (black) showing an ohmic relationship.

From the above findings we explored different buffer layers between the InN and Ge. Aluminum was found to be a good buffer layer material. Every 7^{th} unit cell of Al aligns to within 0.21% to every 8^{th} unit cell of Ge. Every 4^{th} unit cell of InN aligns to every 5^{th} unit cell of Al to within 1%.

A thin epitaxial layer of Al was used as the buffer layer. This construction provides another way for the tandem solar cells to be stacked. It also eliminates the need for a tunnel junction. A tunnel junction requires degenerate doping. Eliminating the need for degenerate doping simplifies the fabrication process of the tandem cell.

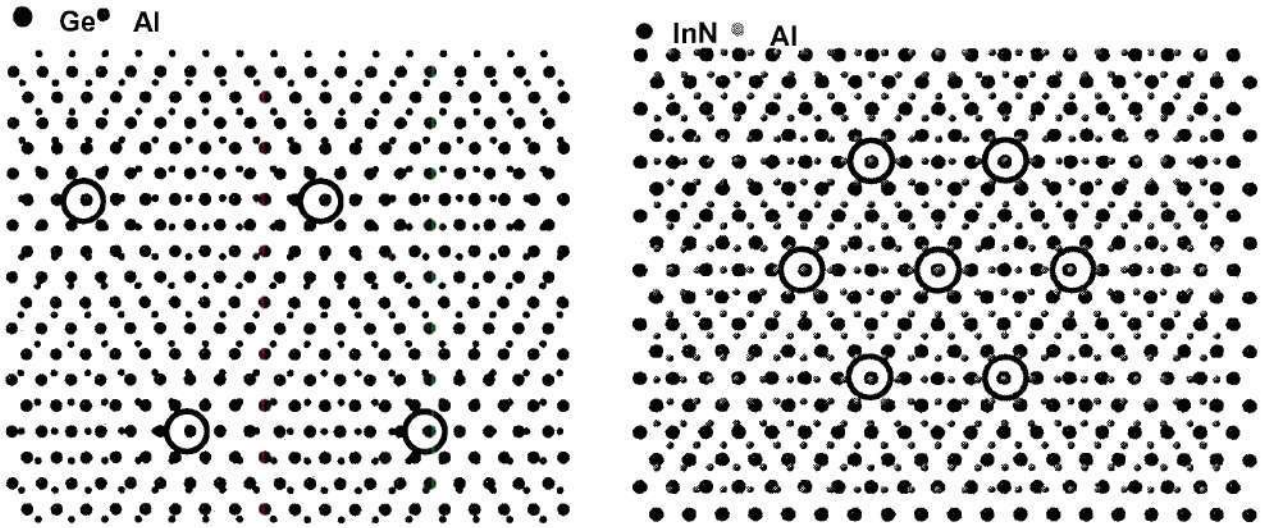

Figure 3: Calculated Schematic showing Lattice Structure of Al Buffer Layer on Ge and InN

During the fall we explored the use of sapphire substrates. InN is more typically grown on sapphire substrates. We wanted to reproduce current results on sapphire to aid in the understanding of InN on Ge. The main discussion point with InN is the bandgap. As reported above our group found a bandgap of InN of 0.69eV on Ge substrates which is consistent with reported results from Davydov and Schaff. Some groups are reporting InN with a bandgap of 1.9eV. We conducted a series of experiments that used different buffer layers between InN and sapphire which would affect the crystalline quality of the film. It was thought that an amorphous InN film might lead to the 1.9eV bandgap. We grew InN/AlN/Sapphire, InN/Nitridation/Sapphire, and InN/Sapphire samples. From X-ray diffraction results we were unable to determine force amorphous phases in the films. We expected that the InN/Sapphire sample would be amorphous, InN/Nitridation/Sapphire sample would be amorphous/crystalline, and the InN/AlN/Sapphire sample would be crystalline. These results did not materialize. However, we were able to find that the quality of the InN film increases with increased thickness. Therefore, a better quality material can be grown with increased growth time. Figure 4 gives X-ray diffraction peaks of two InN films.

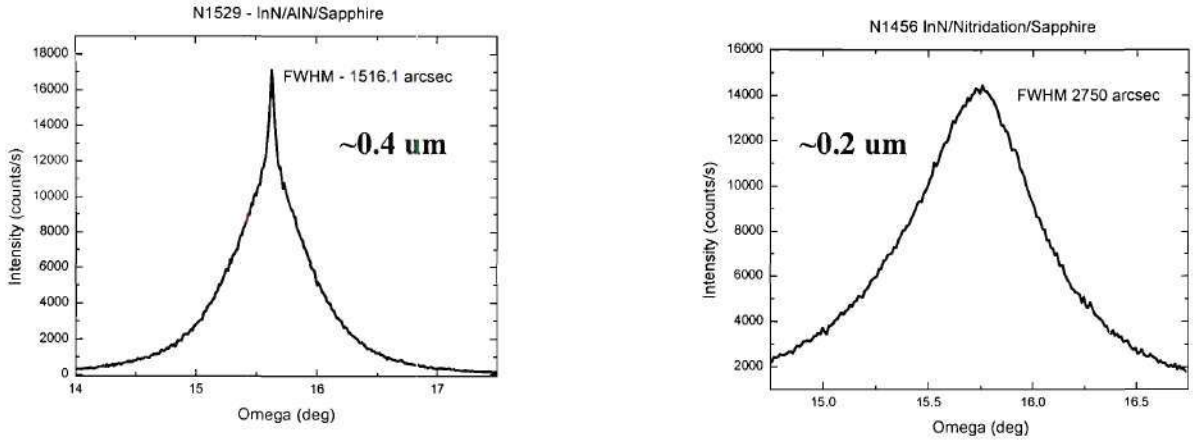

Fig 4: X-Ray Diffraction of InN with Variable Thicknesses

The film on the left was grown for approximately 2 hours where as the film on the right was grown for 1 hour. We believe that the film on the left is a composition of a very disordered film with an ordered film above it. This would lead to the Lorentizan shaped profile.

Additionally, during these sapphire substrate experiments we grew a sample with an Indium Oxide – In_2O_3 film. It was concluded that our MBE machine had a leak which lead to the oxygen contamination. This finding has lead to some interesting results with regards to the bandgap argument. InN and In_2O_3 films have approximately a $\Delta\omega = 0.14^\circ$. Due to this small difference it is probable that the higher InN bandgap was actually the bandgap of an In_2O_3 film. In the following x-ray diffraction diagram it is apparent that there is In_2O_3 in addition to the InN film.

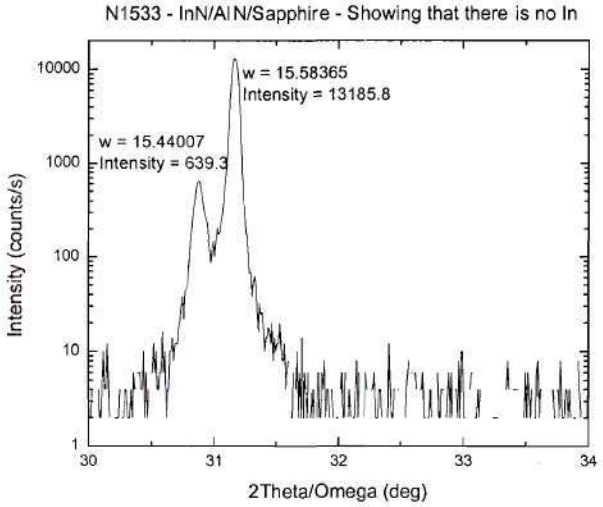

Fig. 5: X-Ray Diffraction of InN film with Presence of In_2O_3

Other samples did not show an In_2O_3 film in the $2\theta/\omega$ scan. However, during a pole figure measurement cubic-In_2O_3 <422> was found. The below figure shows evidence of

hexagonal InN that is 30° rotated with the sapphire substrate and the presence of cubic In_2O_3 (90 degree symmetric peaks pointed to by arrows).

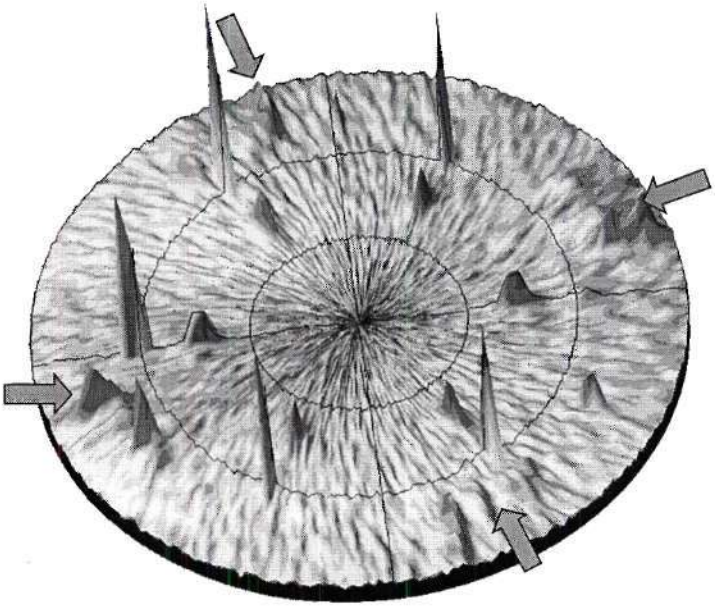

Fig. 6: Pole Figure Measurement of InN Sample

The blue arrows indicate the position of the cubic In_2O_3 film. We believe that this undetected In_2O_3 film has lead to the quoted higher bandgap for InN. To confirm our results SIMS with a Cs ion 15kV primary beam was conducted on a sample with both InN and In_2O_3.

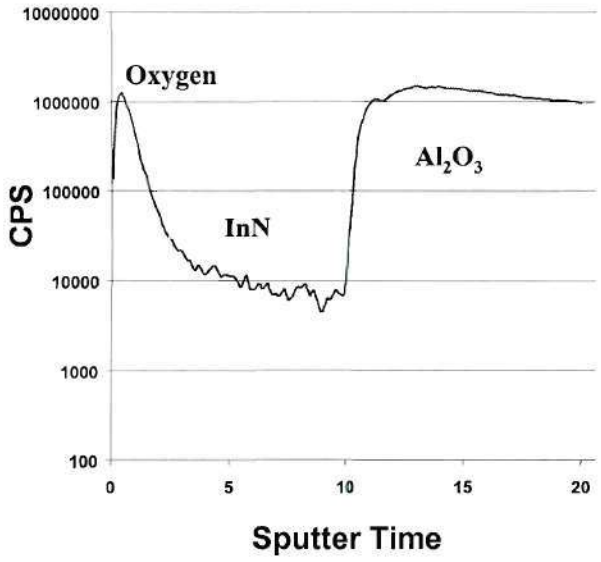

Fig. 7:

From this result we have concluded that the surface of the film will easily oxidize and therefore lead to a higher bandgap material. Finally, we sent samples to The State

University of New York at Buffalo to Dr. Alex Cartwright, where his student Maurice Cheung preformed photoluminescence on a sample that had InN and In_2O_3.

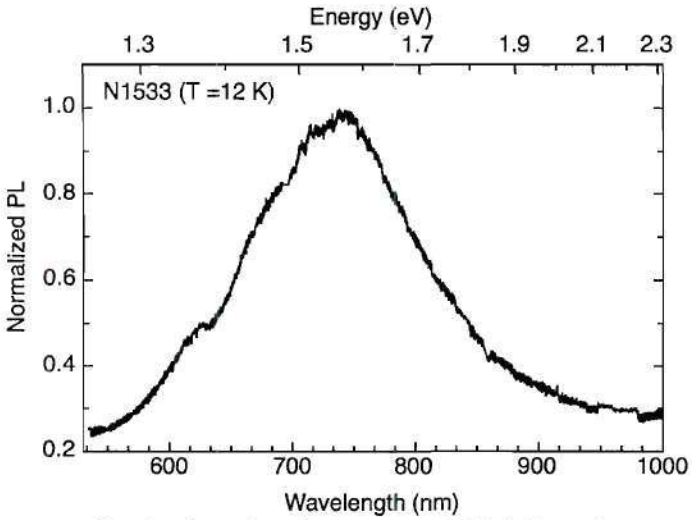

Fig. 8: Photoluminescence of InN Sample

The spectrum itself was difficult to find, because it is overlapped by very strong emission lines from the sapphire substrate. The sharp emission lines were removed to obtain the above plot. The peak is centered at 750nm, which corresponds to approximately 1.6 eV. Compared to the bandgap of InN found for our Journal of Crystal Growth paper of 0.69eV, this emission is closer to 1.9eV value quote by some research groups. In conclusion, we have found results to aid in the discussion of the controversy in the bandgap of InN. Our research shows that the bandgap of InN is correctly found to be ~0.69eV in "clean" "high quality" InN and the larger bandgap of 1.6-1.9eV is related to oxygen content in the InN film , specifically cubic In_2O_3.

Research on InN has lead to the following conclusions and provided guidance towards the direction of our future experiments. InN is a promising and challenging photovoltaic material due to lattice matching of tandem cells, tunnel junctions are a possibility, and epitaxial inter-metallic layers can be used to reduce the previous problems. InN can have a non-stoichiometric, oxygen rich surface layer of the form, cubic In_2O_3. Future efforts will involve doping and heterojunction solar cell development.

High Bandgap InGaN Solar Cells

Two p-i-n and one quantum-well solar cell structures were grown by MOCVD. The quantum-well solar cell consisted of GaN junction and barrier materials with five $In_{0.4}Ga_{0.6}N$ quantum-wells of 1nm thickness in the i-region shown in figure 9. The GaN barriers were 13.8nm thick. The top p-layer thickness was 80nm doped at $2x10^{17}$ cm^{-3}, while the bottom n-layer was 1.5μm thick doped at $4x10^{18}$ cm^{-3} as it also worked as a buffer layer for the i-layer during growth. The GaN buffer layer minimizes the dislocations propagating from the lattice mismatch of the sapphire substrate and GaN into the i-region of the device.

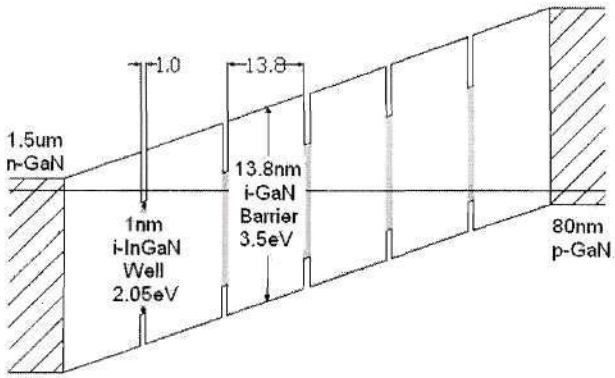

Fig. 9: Band Diagram of Fabricated Quantum-Well Solar Cell

Both the p-i-n devices consisted of 100nm thick $2x10^{17}$ cm^{-3} p-GaN and 200nm thick $4x10^{18}cm^{-3}$ n-GaN. The first p-i-n cell consisted of $In_{0.4}Ga_{0.6}N$ in the i-region. A 1.5μm thick undoped GaN layer was used as a buffer to grow 200nm n-GaN. An undoped GaN layer of 7nm thickness was grown as a buffer to recover the quality of substrate for growth of InGaN. For the $In_{0.4}Ga_{0.6}N$ p-i-n device, the thickness of i-region was limited to 130nm during growth due to possibility of material degradation at a higher thickness. Another similar 7nm thick i-GaN buffer layer was used before growing the top p-GaN layer.

The second p-i-n cell was fabricated with an i-layer of $In_{0.07}Ga_{0.93}N$. $In_{0.07}Ga_{0.93}N$ has a bandgap of 3.1eV and was used to ensure fabrication of a high quality test p-i-n structure to study the behavior of such devices. A top view of completely fabricated structure of this p-i-n cell is shown in figure 10, with the lit area corresponding to light emission from a single device under forward bias.

The material was fabricated into mesa devices by Inductively Coupled Plasma (ICP) Etch. The top of the cell was coated with a thin Ni-Au transparent contact. A 50nm thick p-bonding pad was deposited for external contact. The n-contact consists of 50nm thick Ti-Al-Ti-Au layer. The area of each individual device was 320μm x 320μm as shown in the figure.

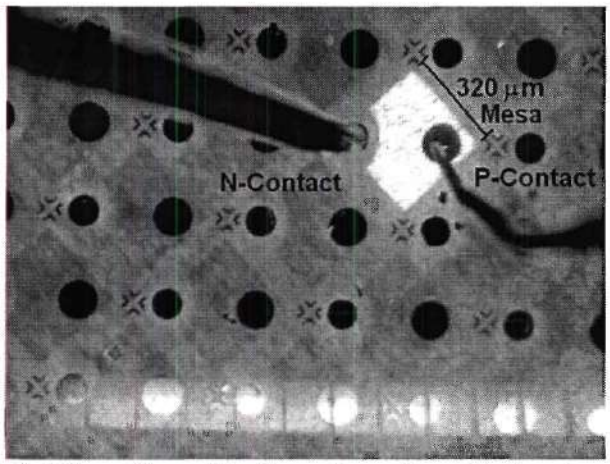

Fig. 10: Fabricated $In_{0.07}Ga_{0.93}N$ p-i-n solar cell mesa structure emitting light at 500nm wavelength at a supply voltage of about 3V

Photoluminescence and x-ray diffraction measurements were performed to characterize the material while I-V and Internal Quantum Efficiency (IQE) measurements were done for electrical characterization of the device.

The I-V measurements were taken under dark conditions, white light as well as in presence of a UV light source. The I-V curve of the quantum-well sample is shown in figure 11. Photo-response of the device to white as well as UV light is seen from the figure. The left shift of the curve under illumination shows an opposing effect of a second diode in series which may be due to the GaN – metal contact interface. The downward shift of the curve under UV illumination shows a significant additional response to UV light.

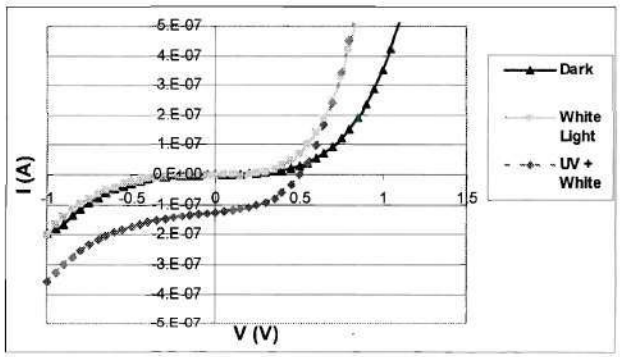

Fig. 11: I-V Curve for Quantum-Well Device under various illuminations

The photoluminescence data from the material used for the QW device at different parts of the sapphire wafer is shown in figure 12.

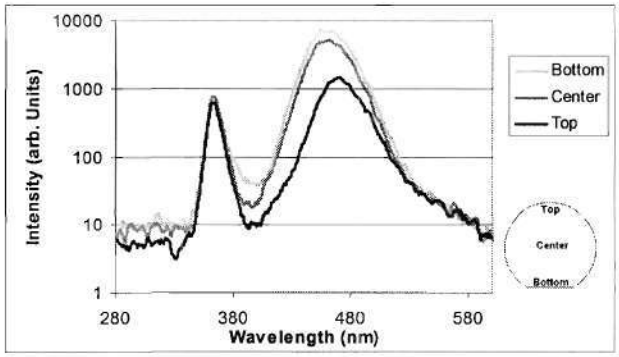

Fig. 12: Photoluminescence for Quantum-Well Device at top, center and bottom of the substrate

Strong photoluminescence peaks are observed at 365nm from GaN and a relatively stronger and broader one at 460nm for the InGaN quantum-wells. Slightly poorer quality growth is observed at the top sites of the wafer as they are situated away form the center of the chamber during the MOCVD growth process.

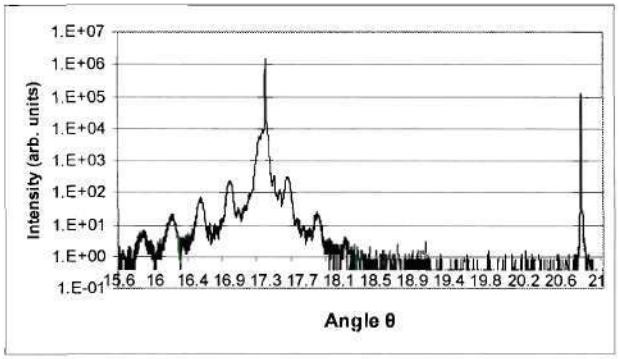

Fig. 13: X-Ray data for Quantum-Well Device.

The quantum-well structures are clearly seen in the X-ray diffraction data in figure 13. The GaN peak is seen at θ=17.28°, while subsequent peaks correspond to the InGaN quantum-well material with 40% In composition and their lower order harmonics. From further analysis, the thickness of the quantum-wells and barriers were confirmed at 1nm and 13.8nm respectively. Moreover, the distinct peaks verify the growth of a good quality crystalline heterostructure.

The I-V curve of the $In_{0.4}Ga_{0.6}N$ p-i-n sample is shown in figure 14. It is seen that the cell hardly responds to white light, while gives a significant response to UV illumination. Again, an opposing diode effect is seen here similar to the quantum-well device most probably due to the Schottky barrier at the GaN-Metal contact interface.

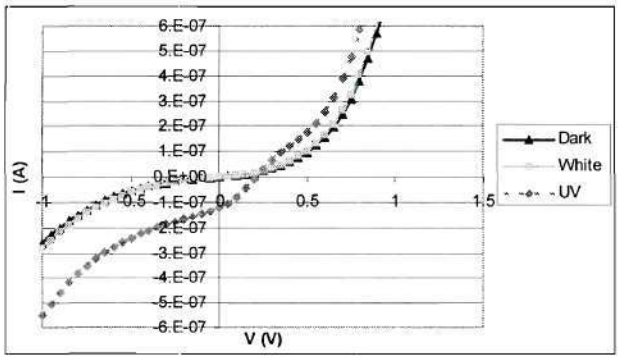

Fig. 14: I-V Curve for p-i-n cell with $In_{0.4}Ga_{0.6}N$ as the i-layer.

Figure 15 shows the x-ray diffraction data for the $In_{0.4}Ga_{0.6}N$ cell. The poor crystalline quality of the material is evident from the graph and reveals a completely relaxed nature of the $In_{0.4}Ga_{0.6}N$ layer. However, the In composition in the material is confirmed at 40%. A poor photoluminescence is also observed for this structure implying a heavily defected material.

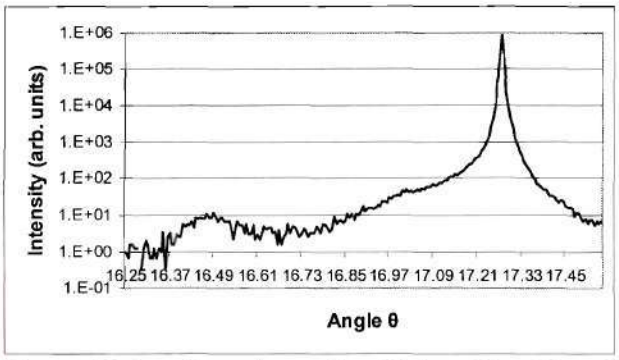

Fig. 15: X-ray -V data for p-i-n cell with $In_{0.4}Ga_{0.6}N$ as the i-layer

The I-V curve of the $In_{0.07}Ga_{0.93}N$ device is shown in figure 16. The bandgap corresponding to InGaN with an In composition of 7% is about 3.1eV. This high bandgap is supported by the marginal response to white light as seen from the I-V curve. The device shows a substantial photo-response UV illumination giving a distinct V_{oc} of 2V.

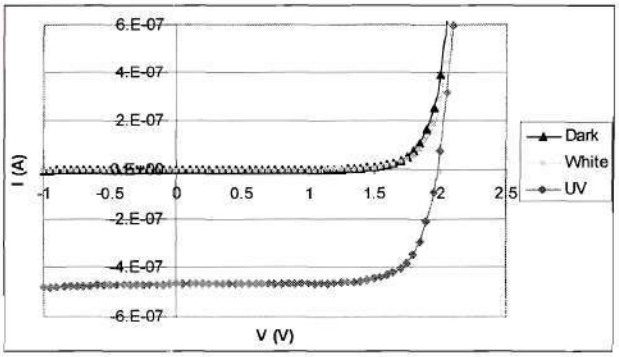

Fig. 16: I -V Curve for p-i-n cell with $In_{0.07}Ga_{0.93}N$ as the i-layer

Emission of green light at 500nm wavelength was observed during the I-V sweep of the device as shown in figure 17. This 500nm corresponds to a bandgap of 2.48 implying the presence of a high quality low bandgap InGaN material with In composition of 27%.

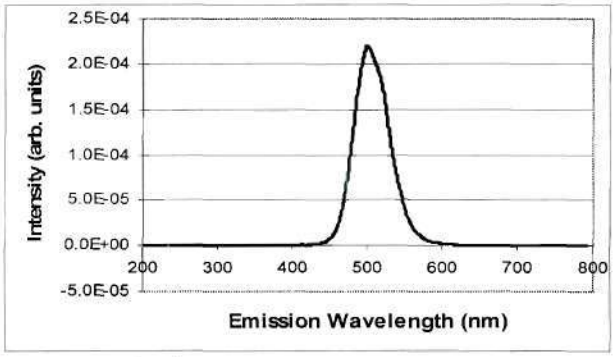

Fig. 17: Emission Spectra of $In_{0.07}Ga_{0.93}N$ p-i-n cell

The photoluminescence data for this device is shown in figure 18. Two PL peaks, a broad peak at 510nm, and a narrower but stronger peak at 500nm, are observed in the spectra. This corresponds to InGaN material with In composition of 27% corresponding to the 500nm emission and that of 28% corresponding to the 510nm emission. No photoluminescence is seen at 400nm wavelength which corresponds to the targeted In composition of 7%.

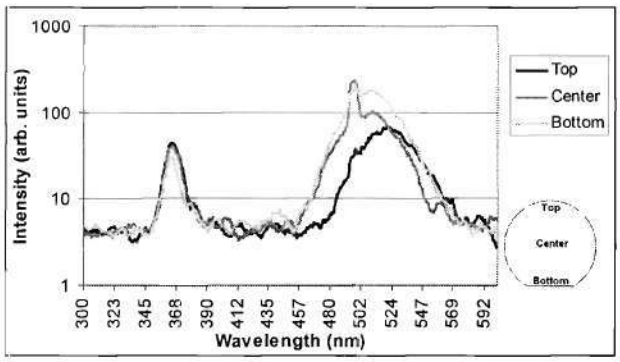

Fig. 18: Photoluminescence Spectra for $In_{0.07}Ga_{0.93}N$ p-i-n device

The X-ray data in figure 19 shows a broad range of In composition in the InGaN i-region. This In composition ranges from 3% to 16% with the maximum intensity at 7%. This peak corresponds to the targeted bandgap of 3.1 eV for the material. A strong peak at θ=17.28° is observed representing good quality GaN.

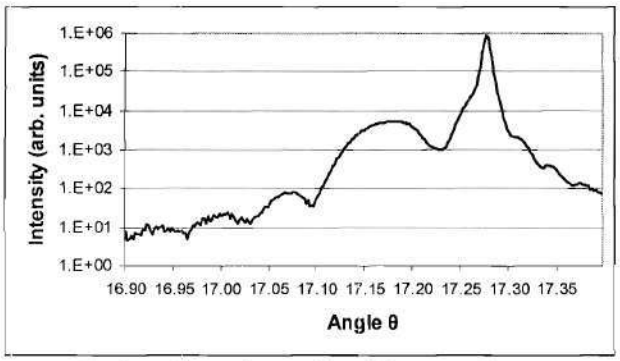

Fig. 19: X-ray -V data for p-i-n cell with $In_{0.07}Ga_{0.93}N$ as the i-layer

Figure 20 shows the IQE data for all the three devices. It can be seen that the $In_{0.4}Ga_{0.6}N$ p-i-n cell has a very weak photo-response due to its poor material quality. This fact is supported by a weak photoluminescence signal and x-ray data. The quantum-well device gives a reflection-corrected QE of 8% at 350nm gradually decreasing till about 470nm under bias light. This bandgap of the semiconductor determined from IQE data is 2.7eV which corresponds to the transition between the first electron and hole energy levels of the $In_{0.4}Ga_{0.6}N$ quantum-well. The low efficiency is primarily due to incomplete absorption of light by the thin wells. An IQE of 19% is observed for the $In_{0.07}Ga_{0.93}N$ p-i-n device. A distinct drop in IQE is seen at 400nm confirming the bandgap of the material at 3.1eV.

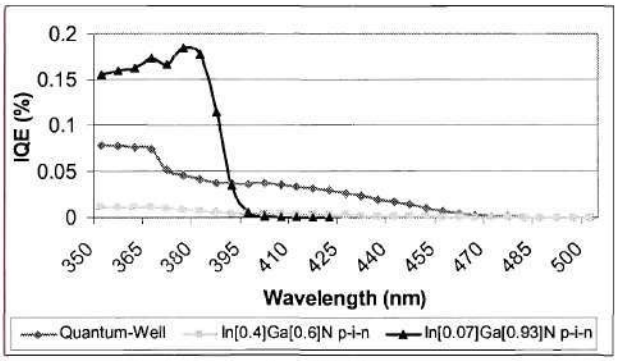

Fig. 20: Internal Quantum Efficiency for (i) Quantum-well, (ii) $In_{0.4}Ga_{0.6}N$ and (iii) $In_{0.07}Ga_{0.93}N$ p-i-n device. Note: Discontinuity at 370nm is due to change in slit width during measurement.

Comparing the results of $In_{0.4}Ga_{0.6}N$ p-i-n and quantum-well structures, the quality in the quantum-well is far more superior as a photovoltaic material than that in the p-i-n structure. This fact is supported by the strong photoluminescence in agreement to the theoretical value of 460nm, a QE of 8% in spite of transmission losses and x-ray diffraction data. Hence, low bandgap InGaN can be incorporated in devices in the form of heterostructures. Moreover, from the response to white light, it can inferred that the quantum-well effective bandgaps can be used to absorb light of very low energy used as bottom cells of ultra-high efficiency tandems.

An opposing current was observed from the I-V curve of the two devices under white light and UV illumination. This is most probably caused by a light activated Schottky contact at the p-GaN - metal interface requiring further investigation.

A high quality p-i-n solar cell was fabricated using the high bandgap $In_{0.07}Ga_{0.93}N$. This fact is supported by the distinct I-V curves and an IQE of 19%. Hence, this high quality crystalline material is an excellent candidate for high performance solar cells.

However, the In-composition in the material is not consistent throughout the structure. This is evident from the x-ray diffraction and photoluminescence and supported by the I-V curves. The x-ray shows a range of In composition in the bulk InGaN centered around the targeted 7%. The IQE also confirms the bandgap of 3.1eV. But the photoluminescence and photoemission peaks show a high quality phase separated InGaN consisting of 27% In. Moreover, this thin layer acts as the recombination site and is responsible for emission of green light from the sample. This phase separated material is consistent with the low Voc of the solar cell at 2V instead of the expected Voc at about 2.6V.

Polarization

The strong polarization of the nitrides offers the potential to overcome some of the limitations of the InGaN system and also to design new solar cell structures. One example of this is an induced junction in the nitrides. Induced junctions use band bending at the interface between two dissimilar materials to invert the surface region, hence giving rise to a junction in the material, but one which does not rely on doping. For materials in which doping is difficult or in which doping introduces defects, an induced

junction can be used instead of a grown or diffused junction. The large piezoelectric coefficients (Fig 21(a) in the III-nitride material system make this a possible solution to the inability to dope the low-band gap compositions of the III-nitride materials. To investigate this possibility, modeling using PC1D was used to simulate the performance of an inverted junction in InN, with the results shown in Fig21(b). These results show that junctions can be formed without requiring doping.

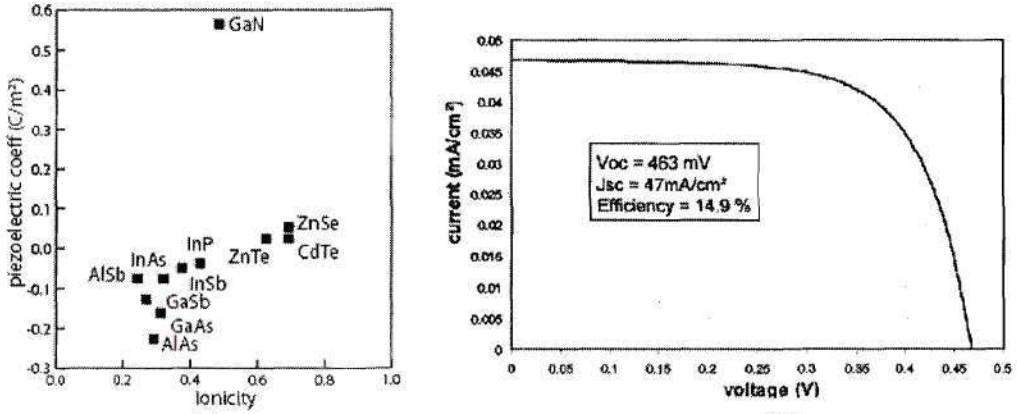

(a) (b)

Fig. 21: (a) Piezoelectric coefficieny after M. Shur of GaN compared to other common semiconductors. (b) IV curve of an induced junction generated by PC1D of a .

Summary

The major achievements for this work include first growth of InN on a Ge substrate.

The other achievement was the first InGaN p-i-n and quantum-well solar cell. In spite of immature technology, a reflection corrected quantum-efficiency of 19% was achieved for the p-i-n cell. High quality MOCVD films for difficult-to-grow materials was demonstrated in the form of superlattices for solar cells. PC1D as well as dedicated code was used to model and design these solar cells.

This work resulted in two invited talks at the 19th European PV SEC and the 31st IEEE PVSC. A paper entitled "Growth of InN on Ge Substrate by Molecular Beam Epitaxy" was submitted to the Journal of Crystal which is currently under review. We are currently in the process of writing a paper of InGaN solar cells for the Journal of Applied Physics.